Comparing the Schrödinger and spinless Salpeter equations for heavy-quark bound states

Steve Jacobs, M. G. Olsson, and Casimir Suchyta III
Physics Department, University of Wisconsin, Madison, Wisconsin 53706
(Received 13 January 1986)

We develop a unified approach to the solution of the Schrödinger and the spinless Salpeter equations. By adjusting the potential and quark masses to best account for the spin-averaged energy levels, we can compare in a realistic way the effect of using a relativistic kinetic energy. Emphasis is given to consideration of relativistic wave-function corrections. We find that the relativistic equation better accounts for the observed energy levels and gives improved results for s- and p-wave annihilation rates and $E1$ transitions.

INTRODUCTION

Potential models have had considerable success in accounting for the observed heavy-quark bound-state spectroscopy.[1-4] Although spin dependence is of intrinsic interest, it necessarily involves additional assumptions within the potential model.[1] Thus, there is some merit in separately analyzing the spin-averaged problem where the Lorentz nature of the potential need not be specified. We employ two QCD-motivated potentials: the Cornell potential[2] for simplicity and the Wisconsin potential,[5] which includes the effects of asymptotic freedom.

We choose as our relativistic equation the spinless Salpeter (SS), or square-root, equation as the most simple generalization of the Schrödinger (S) equation with relativistic kinematics. Since we have little *a priori* knowledge of either the QCD potential or the exact heavy-quark masses, we should not compute relativistic corrections with the same potential and quark masses. With either relativistic (SS) or nonrelativistic wave equations we are attempting to account for the same known state masses and the potential and quark masses are not necessarily the same.

In Sec. I we discuss the wave equations used and their solutions. Details of the method are given in the Appendix. A fit to energy levels and ratios of leptonic widths with the Cornell and Wisconsin potentials is included in Sec. II, and the predicted leptonic and gluonic decays are given in Sec. III. Because the wave functions from short-distance gluon exchanges are singular at the origin, we define an effective wave function at the origin by a sum rule which then can be used in calculating leptonic and gluonic annihilation rates. We also discuss in Sec. III the relativistic corrections to radiative transitions.

I. SPINLESS WAVE EQUATIONS AND THEIR SOLUTIONS

We consider a general coordinate-space wave equation of the form

$$W(-\nabla^2)\psi+V(r)\psi=M\psi \tag{1}$$

for the coordinate difference $\mathbf{r}=\mathbf{r}_1-\mathbf{r}_2$ between the positions of masses m_1 and m_2. For example, in the Schrödinger case,

$$W_S(-\nabla^2)=\frac{-\nabla^2}{2\mu}+m_1+m_2\ . \tag{2}$$

Starting with the Bethe-Salpeter equation,[6] we make a series of approximations consisting of the replacement of the interaction kernel by an instantaneous local potential and the neglect of spin and the coupling of "large-large" to "small-small" components of the wave function. The resulting[7,8] equation is of the form of Eq. (1) with

$$W_{SS}(-\nabla^2)=(-\nabla^2+m_1{}^2)^{1/2}+(-\nabla^2+m_2{}^2)^{1/2}\ . \tag{3}$$

Equations (1) and (3) are called the spinless Salpeter equation. For simplicity in this paper we consider only the equal-mass case in which Eqs. (2) and (3) reduce to

$$W_S=-\frac{1}{m}\nabla^2+2m\ , \tag{4a}$$

$$W_{SS}=2(-\nabla^2+m^2)^{1/2}\ . \tag{4b}$$

The latter equation has the simple virtue of being a direct relativistic generalization of the Schrödinger equation. As mentioned, it is also the spinless approximation to the Bethe-Salpeter equation. Unfortunately, the SS equation is only solvable in closed form for a harmonic-oscillator potential, but numerical solutions are no more difficult to obtain than from the Schrödinger equation.

Our numerical approach will be in momentum space. The reason for this is that wave functions are well behaved whereas in coordinate space there is a well-known relativistic wave-function singularity at $r=0$ for a singular (e.g., Coulombic) potential due to the usual instantaneous approximation. In addition, the coordinate-space $(v/c)^2$ expansion—the Breit-Fermi interaction—is quite singular, a problem not present in momentum space. Finally, in our solution method an integral equation in momentum space is no more difficult to solve than the differential form of Schrödinger's equation in coordinate space.

Transforming Eq. (1) to momentum space we obtain

$$W(p^2)\hat{\psi}+\hat{V}_*\hat{\psi}=M\hat{\psi}\ , \tag{5}$$

where the caret denotes the Fourier transform and the asterisk denotes convolution:

$$g_1*g_2\equiv\int\frac{d^3\mathbf{p}'}{(2\pi)^3}g_1(\mathbf{p}-\mathbf{p}')g_2(\mathbf{p}')\ . \tag{6}$$

In momentum space, the only difference between the Schrödinger and the relativistic equations is in the multiplicative function $W(p^2)$. We solve Eq. (5) using the Rayleigh-Ritz-Galerkin method; details are given in the Appendix. The approximate eigenvalues will be in the eigenvalues of the matrix A whose elements are

$$A_{ij}=\langle\hat{e}_i,W(p^2)\hat{e}_j\rangle+\langle\hat{e}_i,\hat{V}_*\hat{e}_j\rangle\ , \tag{7}$$

where the angle brackets denote the inner product

$$\langle g_1,g_2\rangle\equiv\int d^3\mathbf{p}\,g_1(\mathbf{p})g_2(\mathbf{p})\ , \tag{8}$$

and the $\{\hat{e}_i\}$ are an orthonormal complete set of functions in momentum space. The second inner product in Eq. (7) may be simply evaluated by noting that

$$\begin{aligned}\langle\hat{e}_i,\hat{V}_*\hat{e}_j\rangle&=\langle\hat{e}_i,[V(r)e_j(\mathbf{r})]\hat{\ }\rangle\\&=(2\pi)^3\langle e_i(-\mathbf{r}),V(r)e_j(\mathbf{r})\rangle\ ,\end{aligned} \tag{9}$$

where $e_i(\mathbf{r})$ is the inverse transform of $\hat{e}_j(\mathbf{p})$. The complete set of basis functions $\{e_i\}$ is arbitrary except that for reasons of simplicity it is highly desirable that the e_i have analytic Fourier transforms and that their energy eigenvalues are discrete. The latter condition would, for example, eliminate hydrogenic wave functions. An obvious candidate for the set of basis functions is the harmonic-oscillator wave functions.[6] We have chosen an alternate set which more closely resembles hydrogenic wave functions. Our set is related to Jacobi polynomials in momentum space and Laguerre polynomials in coordinate space. The basis functions are eigenstates of orbital angular momentum and have the correct threshold behavior explicitly factored out. Again, we refer to the Appendix for a more complete discussion.

II. COMPARING WITH EXPERIMENT

Since the wave equations we are considering have no spin we compare our predictions to spin-averaged energy levels and to ratios of leptonic widths.[4,5] For a given form of the interquark potential we will vary the potential parameters and quark masses to achieve the best possible agreement with the experimental data, considering separately the S and SS wave equations. We will investigate two successful QCD-motivated potential forms.

A. Cornell potential

The Cornell potential is the simplest of the QCD-motivated potentials:

$$V_C(r)=-\frac{\kappa}{r}+ar\ , \tag{10}$$

where $\kappa=\frac{4}{3}\alpha_s$ is supposed to represent short-range gluon exchange and a is the confinement string tension. The main drawback of this potential is that the $c\bar{c}$ and $b\bar{b}$ states lie in an intermediate region of quark separation where neither limiting forms in Eq. (10) should be valid. The fact that this potential works reasonably well is an indication that there is a smooth transition between the perturbative and nonperturbative regimes. In Table I we list the $c\bar{c}$ and $b\bar{b}$ spin-averaged bound-state data below open flavor threshold.

We vary potential parameters κ and a along with the quark masses m_c and m_b to optimize agreement to the data of Table I. First we use the Schrödinger wave equation and then the relativistic spinless Salpeter equation. In each case the fit to the data is quite good with the possible exception of the lowest spin-averaged χ_c state, the $1P$; the fits are both about 30 MeV too low.

Although we have commented on this $1P$ difficulty previously,[4] we might briefly remind the reader why the difficulty was not evident to earlier workers in this area. We use spin-averaged levels in which the $1S$ and $2S$ $c\bar{c}$ masses are about 30 MeV below the ψ and ψ' states, respectively. The $1P$ level, on the other hand, is near the center of gravity (c.o.g.) of the χ_J states since the p-wave hyperfine splitting is probably small. Previous work has used the $\psi,1P,\psi'$ masses giving a misleadingly satisfactory agreement with experiment.

The effective potential for each wave equation is plotted in Fig. 1. In the relativistic fit, the string tension is slightly larger while the color coupling constant α_S is slightly smaller so the SS potential exceeds the S potential

TABLE I. Fit to spin-averaged levels and ratios of leptonic widths using the Cornell potential. Level energies are in MeV. The potential parameters and quark masses were varied to best account for the data. The data set is discussed in Refs. 4 and 5. Both nonrelativistic kinetic energy (Schrödinger) and relativistic kinetic energy (Salpeter) wave equations were tried.

	Data	Schrödinger	Salpeter
	$c\bar{c}$		
M_{1S}	3068±2	3069	3069
M_{1P}	3531±10	3500	3506
$\Gamma_{ee}(\Psi')/\Gamma_{ee}(\Psi)$	0.45±0.06	0.50	0.56
M_{2S}[a]	3633±2	3697	3667
	$b\bar{b}$		
M_{1S}	9442±10	9445	9445
M_{1P}	9900±6	9897	9903
M_{2S}	10014±10	10004	10000
M_{2P}	10256±5	10259	10263
M_{3S}	10346±10	10354	10350
$\Gamma_{ee}(\Upsilon')/\Gamma_{ee}(\Upsilon)$	0.44±0.03	0.41	0.44
$\Gamma_{ee}(\Upsilon'')/\Gamma_{ee}(\Upsilon)$	0.335±0.03	0.30	0.33
χ^2		20.6	21.2
	Fit parameters		
κ		0.471	0.446
a (GeV)^2		0.192	0.200
m_c (GeV)		1.320	1.327
m_b (GeV)		4.746	4.737

[a]Not included in fit.

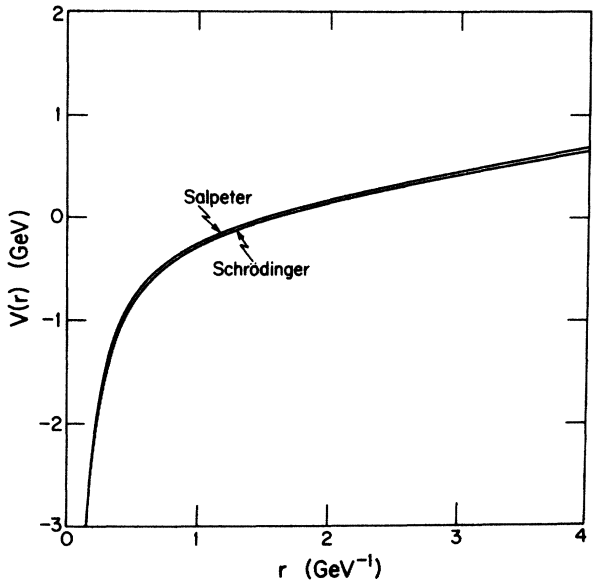

FIG. 1. Potentials of the Cornell form, which best fit the heavy-quark data using nonrelativistic (Schrödinger) and relativistic (spinless-Salpeter) wave equations

at each quark separation. As pointed out by Durand and Durand,[8] this is what one would expect, since for a given momentum the relativistic kinetic energy is less than the nonrelativistic kinetic energy. If the energy levels are kept fixed, the relativistic potential energy must then exceed the nonrelativistic potential energy. The difference between the potentials is suppressed to some extent because we have required leptonic width ratios as well as the energy levels to agree. In addition, the Durands conjecture[8] that for a confining potential this means a more confined wave function and hence an enhanced annihilation decay rate. We shall verify this by direct calculation in Sec. III.

Finally, let us try to accommodate $s\bar{s}$ states within this scheme. One might expect that the effective color coupling constant for $s\bar{s}$ states is larger than that for $c\bar{c}$ so we introduce a separate coupling constant κ_s. The $s\bar{s}$ states we try to fit are the $1S$(1.00 GeV) and the $2S$(1.61 GeV). The $1S$ level is the spin-averaged η'(0.958) and ϕ(1.020) states and the $2S$ level is obtained by spin averaging the i(1.440) and ϕ(1.680) states. The results are shown in Table II. The relativistic wave equation works much better than the nonrelativistic Schrödinger equation but still overestimates the $2S$ mass. The κ_s parameter is smaller in the SS fit, and also a small strange-quark mass is indicated although since its kinetic energy far exceeds its rest energy the strange-quark mass is poorly determined.

B. Wisconsin potential

We also consider a more realistic potential[5] which exhibits the full content of perturbative QCD at short distance, linear confinement at a large distance, and flexible phenomenological parametrization at intermediate range. This potential has the form

TABLE II. If the data set of Table I is expanded to include $s\bar{s}$ states we find that the relativistic wave equation is significantly superior. The Coulombic coupling constant is larger as expected qualitatively from QCD. The level energies are in MeV.

	Data	Schrödinger	Salpeter
		$s\bar{s}$	
M_{1S}	1004	999	1002
M_{2S}	1615	2016	1735
		Fit parameters	
κ_s		1.8	0.87
m_s (GeV)		0.39	0.07

$$V_W(r)=V_S(r)+V_I(r)+V_L(r)\ , \tag{11}$$

where the short-range potential V_S is a regularized version[5] of the two-loop perturbative potential in which the Landau zero is pushed off to infinity. The intermediate potential V_I is taken to be $V_I(r)=r(c_1+c_2r)e^{-r/r_0}$, a rather arbitrary choice whose only requirement is that it vanishes at small and large quark separations. The long-range potential is the usual $V_L(r)=ar$ linear confinement.

It is important that the choice of the phenomenological potential be consistent with the desired perturbative result. This will be difficult if V_I and V_L are significant for small r. Another requirement should be that there is no stiff coupling of the perturbative short-range potential to the longer-range potential. If this were the case, the physical data would enforce a strong relation between the perturbative potential and longer distances where the $c\bar{c}$ and $b\bar{b}$ states primarily lie. This, for example, would imply an unrealistically accurate determination of the perturbative scale parameter $\Lambda_{\overline{\rm MS}}$, where $\overline{\rm MS}$ is the modified minimal subtraction scheme. In this potential,[5] we avoid both pitfalls by assigning an error to the potential as a function of radius based upon an estimate of the α_s^3 term neglected in the perturbative calculation. This error grows with increasing radius so that the asymptotic-freedom requirement becomes weaker as the quarks separate and a smooth transition from the perturbative regime is achieved.

As before, we vary the parameters of the Wisconsin potential and the heavy-quark masses to optimize the agreement with the spin-averaged data but with the additional constraint that the potential approximates the perturbative result in its range of applicability. The result for both S and SS wave equations is very good. The detailed comparison with the data is given in Table III. A fit to the $s\bar{s}$ states using the Wisconsin potential gives somewhat better results than in Table II with the Cornell potential.

III. WAVE-FUNCTION CORRECTIONS

Knowledge of accurate heavy-quark bound-state wave functions is required to evaluate transition rates. These transitions are of two types: (i) annihilation into leptons,

photons, or light quarks and (ii) radiative decay into another heavy-quark bound state by emission of photons or light mesons. The radiation of photons is computed by the evaluation of an expectation value. This evaluation is quite straightforward for either Schrödinger or spinless Salpeter wave functions since the integrand vanishes at the origin where the instantaneous approximation breaks down. The calculation of annihilation rates, on the other hand, requires wave-function values at small quark separations. When a relativistic equation, with a strongly attractive short-range potential, is solved in the usual instantaneous approximation the wave function at the origin is singular or at least anomalously large. Retardation effects are expected to modify these short-distance singularities.[7] Instantaneous wave functions from singular potentials therefore have unphysical short-distance behavior and we must take care to define what is meant by the annihilation rate.

Some wave functions resulting from the calculations of the last section are displayed in Figs. 2–9. Figures 2–5 show the wave functions for the $1S$, $1P$, and $2S$ states for the Cornell potential. Each figure depicts the results for the $c\bar{c}$ and $b\bar{b}$ systems. The dashed lines are the S wave functions and the solid curves the SS wave functions.

A heavy-quark system is nearly nonrelativistic near the classical turning point so it is not surprising to see that the wave functions for the S and SS equations are similar in this region. The S and SS wave functions differ most markedly within about two Compton wavelengths where the relativistic wave function rises above[8] the Schrödinger one. Within about one-fifth Compton wavelength we see evidence of singular behavior.[9] Since our basis function set is regular at $r=0$, we see successively better approximations to the singularity as we use 5, 10, or 20 basis functions. Because the wave function at the origin is not well defined we cannot directly apply the SS wave functions in calculating annihilation rates. The corresponding wave functions using the Wisconsin potential are given in Figs. 6–9.

Since the above instantaneous relativistic wave func-

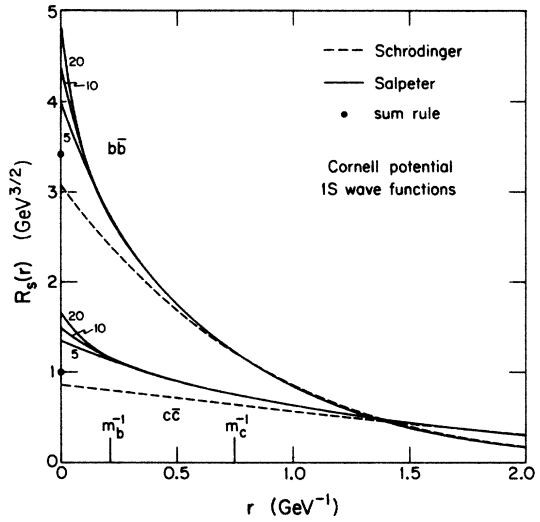

FIG. 2. $1S$ wave functions using the Cornell potential. The instantaneous relativistic Salpeter solution shows singular behavior at the origin as seen by the increase as the number of basis functions is increased. The dots show the sum rule of Eq. (12) for the effective $|R_s(0)|^2$ from the SS wave function

TABLE III. Fit to spin averaged levels and ratios of leptonic widths using the Wisconsin potential. Level energies are in MeV. The potential parameters and quark masses were varied to best account for the data; see Refs. 4 and 5. Both nonrelativistic kinetic energy (Schrödinger) and relativistic kinetic energy (Salpeter) wave equations were tried. $\Lambda_{\overline{MS}}=250$ MeV.

	Data	Schrödinger	Salpeter
	$c\bar{c}$		
M_{1S}	3068±2	3069	3069
M_{1P}	3531±1	3503	3513
$\Gamma_{ee}(\Psi')/\Gamma_{ee}(\Psi)$	0.45±0.06	0.47	0.47
M_{2S}[a]	3663±2	3682	3657
	$b\bar{b}$		
M_{1S}	9442±10	9439	9437
M_{1P}	9900±6	9890	9894
M_{2S}	10014±10	10022	10021
M_{2P}	10256±5	10244	10247
M_{3S}	10346±10	10357	10354
$\Gamma_{ee}(\Upsilon')/\Gamma_{ee}(\Upsilon)$	0.44±0.03	0.40	0.41
$\Gamma_{ee}(\Upsilon'')/\Gamma_{ee}(\Upsilon)$	0.335±0.03	0.31	0.33
χ^2		27.4	14.0
	Fit parameters		
a (GeV^2)		0.204	0.206
c_1 (GeV^2)		−1.23	−1.25
c_2 (GeV^3)		1.08	1.09
r_0 (GeV^{-1})		0.681	0.671
m_c (GeV)		1.441	1.467
m_b (GeV)		4.852	4.860

[a]Not included in fit.

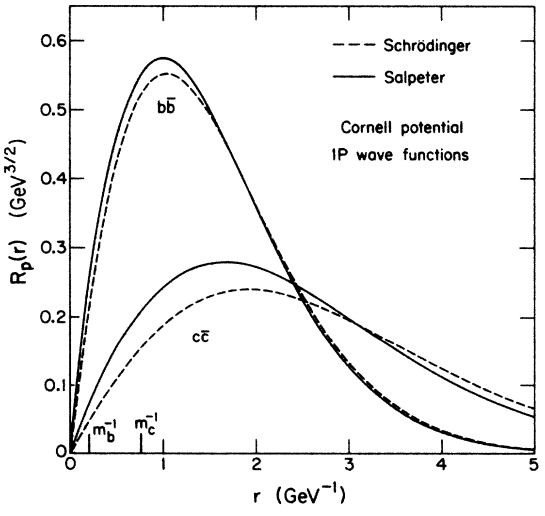

FIG. 3. $1P$ wave functions using the Cornell potential.

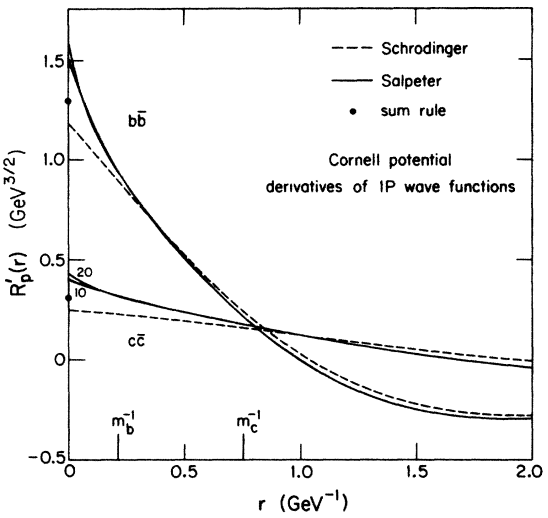

FIG. 4. Derivative of the $1P$ wave functions using the Cornell potential. The dots represent the sum-rule calculation of Eq. (13) for the effective value of $|R_p'(0)|^2$.

tions are poorly defined at the origin we must consider methods to reinterpret these results for the calculation of annihilation. In lieu of a more exact calculation including retardation, some sort of "smearing" has been employed by previous authors. In coordinate space one can smear either the wave function or the potential over some small volume roughly a Compton wavelength in size. The guiding idea is that annihilation will occur within a Compton wavelength in a correct relativistic theory. Unfortunately, the exact radius chosen is critical as can be seen from the wave-function figures. If a smearing radius of two Compton wavelengths is adopted, the relativistic and nonrelativistic results will be virtually identical since the volume element emphasizes the largest radius. In addition, there is no clear nonrelativistic limit in this smearing scheme.

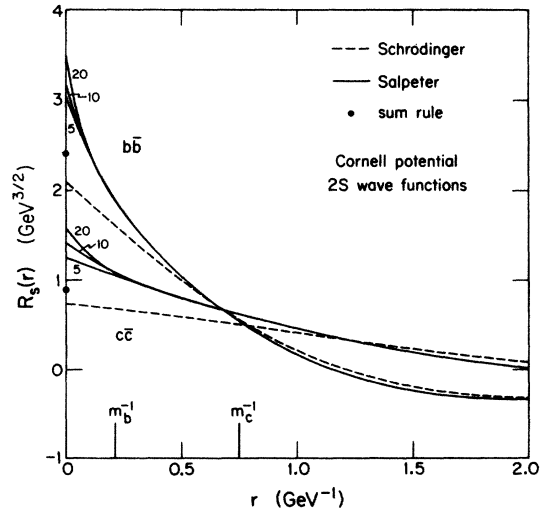

FIG. 5. $2S$ wave functions using the Cornell potential. The singular nature of the wave function is suggested by the variation as the number of trial wave functions increases.

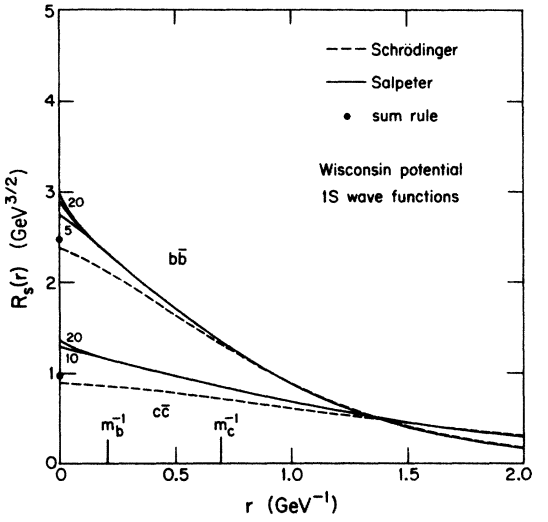

FIG. 6. $1S$ wave functions for the Wisconsin potential. (See Fig. 2.)

One can also smear in momentum space. One procedure which can be adopted[10] is to introduce a cutoff function such as $(1+p^2/m^2)^{-1/2}$ in the momentum-space wave function. The Fourier transform wave function is then finite at $r=0$ and the nonrelativistic limit is built in. As one might expect, the resulting wave function at the origin is quite sensitive to the cutoff function.

We have adopted a smearing procedure based closely on the nonrelativistic nature of the problem at large radii. Starting from the Schrödinger equation, integrating by parts and applying the usual boundary conditions at $r=0$ and ∞ we have,[11] for $l=0$,

$$|R_s(0)|^2 = m_Q\left\langle \frac{dV}{dr}\right\rangle \tag{12}$$

and, for $l=1$,

$$|R_p'(0)|^2 = \frac{m_Q}{9}\left\langle \frac{1}{r^2}\frac{dV}{dr} + \frac{4(E-V)}{r^3}\right\rangle , \tag{13}$$

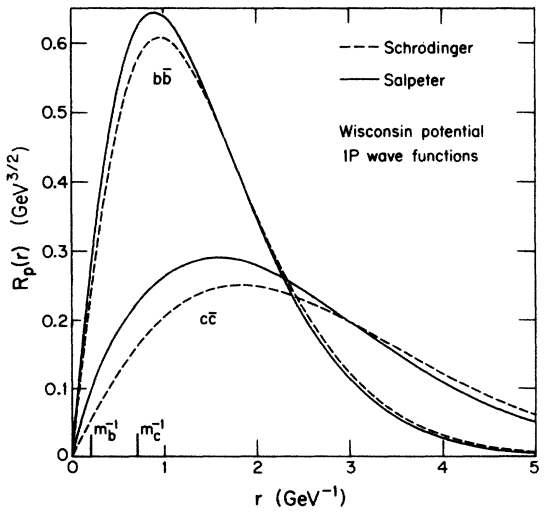

FIG. 7. $1P$ wave functions with the Wisconsin potential.

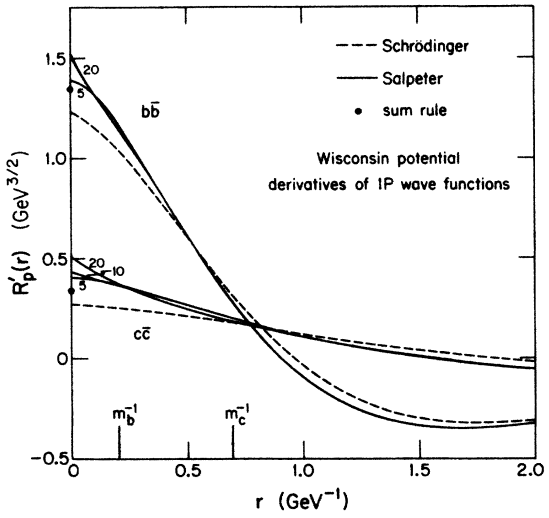

FIG. 8. Derivative of the $1P$ wave function using the Wisconsin potential. (See Fig. 4.)

where $E=M_{Q\bar{Q}}-2m_Q$. For the Schrödinger equation, Eqs. (12) and (13) are identities. For the SS equation these sum rules define effective wave-function values at the origin. The effective values are computed as expectation values using the corresponding instantaneous wave functions. Analogous relations can be found for higher angular momentum states. In Figs. 2, 4–6, 8, and 9 the sum-rule values of Eqs. (12) and (13) are indicated.

In the remainder of this section we investigate the effects of relativistic corrections on leptonic, radiative, and gluonic widths.

A. Leptonic widths

The ratios of leptonic widths were used in the fits and as seen from Tables I and III are satisfactorily accounted for for both potentials and both wave equations. In ratios the radiative gluonic corrections are thought to cancel. In this subsection we consider the absolute values of the leptonic widths. The leptonic width including second-order radiative corrections[8] is

$$\Gamma_{ee}(^3S_1)=\Gamma_{ee}^{(0)}(1-\Delta)\,,$$
$$\Gamma_{ee}^{(0)}=\frac{4\alpha^2 e_Q^{\,2}}{M^2}\,|R_s(0)|^2\,, \tag{14}$$
$$\Delta\simeq\frac{16}{3}\left[\frac{\alpha_s}{\pi}\right]-(24.26-0.11n_f)\left[\frac{\alpha_s}{\pi}\right]^2\,.$$

Numerically, the radiative correction term Δ is

$$1-\Delta=\begin{cases}0.76, & \alpha_s=0.20,\ n_f=3\,,\\ 0.79, & \alpha_2=0.16,\ n_f=4\,.\end{cases} \tag{15}$$

The upper value was used for the ψ while the lower one was used in correcting the Υ leptonic widths. From Figs. 2 and 6 we can read off the S and effective SS wave functions at the origin. The predicted absolute leptonic widths are given in Table IV. Taking into account the uncertainties in the gluonic radiative correction, all of these values are reasonable. The somewhat large Υ leptonic widths predicted by the Cornell potential is presumably due to the stronger Coulomb singularity in the potential compared to the logarithmically modified singularity in the asymptotically free Wisconsin potential.

B. Radiative transitions

As we indicated earlier, radiative transitions between heavy states are well defined even in the instantaneous approximation. We will discuss here the spin-independent relativistic correction to the electric dipole transitions occurring between sharp states in the $c\bar{c}$ and $b\bar{b}$ spectroscopies. The transitions observed so far are of the type

$$\Gamma(^3S_1\to{}^3P_J\gamma)=\frac{4\alpha(2J+1)k^3e_Q^{\,2}\,|\langle{}^3P_J\,|\,r\,|\,{}^3S_1\rangle|^2}{27} \tag{16a}$$

and

$$\Gamma(^3P_J\to{}^3S_1\gamma)=\frac{4\alpha k^3 e_Q^{\,2}\,|\langle{}^3S_1\,|\,r\,|\,{}^3P_J\rangle|^2}{9}\,, \tag{16b}$$

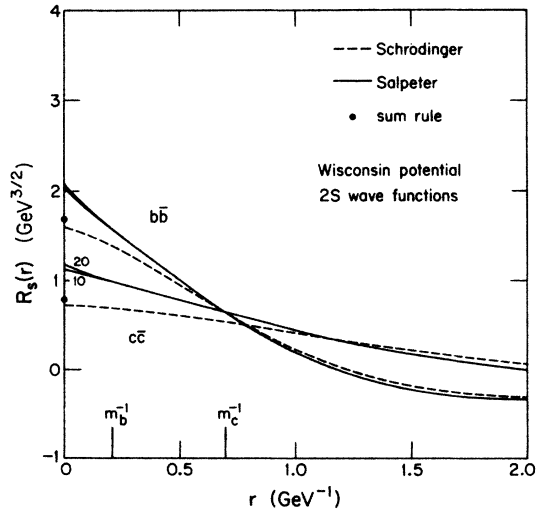

FIG. 9. $2S$ wave function from the Wisconsin potential. (See Fig. 5.)

TABLE IV. Leptonic widths for ψ and Υ states predicted by our potentials and wave equations. The radiative corrections of Eq. (14) are qualitatively correct.

	Cornell		Wisconsin	
	S	SS	S	SS
$c\bar{c}$	$\Gamma_{ee}(1S)=4.60\pm0.39$ keV (experiment)			
$\lvert R_{1S}(0)\rvert^2$ (GeV^3)	0.74	1.00	0.79	0.94
$\Gamma_{ee}^{(0)}$ (keV)	5.60	7.60	6.00	7.10
$\Gamma_{ee}^{(0)}(1-\Delta)$ (keV)	4.30	5.80	4.60	5.40
$b\bar{b}$	$\Gamma_{ee}(1S)=1.10\pm0.12$ keV (experiment)			
$\lvert R_{1S}(0)\rvert^2$ (GeV^3)	9.4	11.6	5.6	6.2
$\Gamma_{ee}^{(0)}$ (keV)	1.9	2.3	1.1	1.2
$\Gamma_{ee}^{(0)}(1-\Delta)$ (keV)	1.5	1.8	0.9	0.95

where the notation $^3S_1$ or ^3P_J might denote any radially excited state. The quark charge e_Q is in units of the electronic charge and k is the c.m. photon energy. Spin-independent relativistic corrections are automatically included if relativistic wave functions are used as shown by Siegert's theorem.[12]

The predicted $E1$ transition rates for the sharp $^3S_1$ and $^3P_2$ states are given in Table V for the Cornell and Wisconsin potentials using the Schrödinger and spinless Salpeter wave equations. We first note that in the well-determined cases, relativistic kinetic energy corrections reduce the radiative widths by 5–20%. However, contrary to conventional wisdom,[12] transitions involving wave functions with the same number of nodes are more strongly affected by these relativistic corrections. In particular, the $\psi' \to \chi_2 \gamma$ transition width is decreased by the relativistic kinetic energy correction but by less than 15%, not enough to agree with the experimental value which is about half the nonrelativistic prediction. Spin-dependent corrections and admixture of $D\bar{D}$ states may also be important.

In Table V we also have computed an "average" width which is taken over the two potential forms and with nonrelativistic and relativistic kinetic energies. The error assigned to this average encompasses the individual values. The average value thus gives an estimate for a model-independent transition width. Unfortunately, there is little experimental information yet available for $b\bar{b}$ radiative transitions.

C. Hadronic total widths

Some of the earliest QCD predictions[13] were made for the hadronic widths of heavy quark bound states. In standard $^{2S+1}L_J$ spectroscopic notation, the lowest-order hadronic widths, denoted by the minimum number of gluons, are

$$\Gamma(^1S_0 \to 2g) = \frac{8\alpha_s^2}{3M^2} |R_s(0)|^2 , \tag{17a}$$

$$\Gamma(^3S_1 \to 3g) = \frac{40(\pi^2-9)\alpha_s^2}{81M^2} |R_s(0)|^2 , \tag{17b}$$

$$\Gamma(^3P_0 \to 2g) = \frac{96\alpha_s^2}{M^4} |R_p'(0)|^2 , \tag{17c}$$

$$\Gamma(^3P_1 \to 3g;q\bar{q}g) = \frac{128\alpha_s^3}{3\pi M^4} |R_p'(0)|^2 \ln\left[1-\frac{M^2}{4m_Q^2}\right]^{-1} , \tag{17d}$$

$$\Gamma(^3P_2 \to 2g) = \tfrac{4}{15}\Gamma(^3P_0 \to 2g) , \tag{17e}$$

$$\Gamma(^1P_1 \to 3g;q\bar{q}g) = \tfrac{5}{6}\Gamma(^3P_1 \to 3g;q\bar{q}g) . \tag{17f}$$

In these annihilation rates either the s-wave function at the origin or the derivative of the p-wave wave function at the origin must be specified. We will consider directly the Schrödinger wave function at the origin for the Cornell and Wisconsin potentials. For the corresponding solutions to the SS equation we use the sum rules of Eqs. (12) and (13) in calculating the annihilation rates.

We concentrate on the two gluon decays of the η_Q and χ_{JQ} states. Three gluon decays of $^3S_1$ states are reviewed by Lepage.[14] For two gluon decays it has been pointed out recently[15] that the lowest-order formulas seem to work best for the η_c and χ_b states while considerably underestimating the χ_c widths. Although this discrepancy may have a number of possible explanations we will consider here only relativistic spin-independent wave-function corrections. We also briefly discuss why some other effects are not important.

First we consider pseudoscalar ($^1S_0$) decays into two gluons. Using Eq. (17a) and the wave functions of Table IV we calculate the ground-state η_Q widths in Table VI. The η_c width has been measured[16] to be $\Gamma(\eta_c \to \text{all}) = 11.5^{+4.5}_{-4.0}$ MeV. For $\alpha_s = 0.2$ the predictions are all consistent with this value. As seen in Table VI, the predicted η_b width is comparable to the η_c width. The decrease of an order of magnitude due to the M^{-2} factor is compensated by an increase in the wave function at the origin.

The χ_{2Q} decays into two gluons in lowest order are computed with the aid of Eqs. (17c) and (17e). The wave functions for each of our potentials and wave equations are given in Table VII. There is some experimental evi-

TABLE V. Electric dipole radiative widths (in keV) involving $^3S_1$ and χ_2 states. The relativistic wave equation reduces the $\psi' \to \chi_2\gamma$ rate by about 13%. The "no node" transition $\chi_2 \to \psi\gamma$ is reduced by 20%.

Process	Cornell		Wisconsin			
	S	SS	S	SS	Average	Experiment
			$c\bar{c}$ widths			
$\chi_2 \to \psi\gamma$	577	475	515	419	497±80	330±170
$\psi' \to \chi_2\gamma$	36	31	35	31	33±3	17±5
			$b\bar{b}$ widths			
$\chi_2 \to \Upsilon\gamma$	37	35	39	36	37±2	
$\Upsilon' \to \chi_2\gamma$	2.3	2.2	2.0	1.9	2.1±0.2	
$\chi_2' \to \Upsilon'\gamma$	18	16	21	20	19±3	
$\chi_2' \to \Upsilon\gamma$	12	11	10	8	10±2	
$\Upsilon'' \to \chi_2'\gamma$	2.6	2.5	2.3	2.2	2.4±0.2	
$\Upsilon'' \to \chi_2\gamma$	0.3	0.7	0.03	0.003	0.4±0.4	

TABLE VI. Pseudoscalar widths (in MeV). Since the wave equation at the origin increases to compensate for the decreased m^{-2} factor in Eq. (17a) the η_b and η_c widths are comparable.

	Cornell		Wisconsin	
	S	SS	S	SS
$\Gamma(\eta_c \to 2g) = 11.5^{+4.5}_{-4.0}$ MeV (experiment)				
	$\Gamma(\eta_c \to 2g)$ (MeV)			
$\alpha_s = 0.2$	9.0	12.2	9.6	11.5
	$\Gamma(\eta_b \to 2g)$ (MeV)			
$\alpha_s = 0.16$	7.2	8.8	4.3	4.7
$\alpha_s = 0.18$	9.1	11.1	5.4	5.9

dence[17–19] for χ_{2b}, χ'_{2b}, and χ_{2c} two gluon widths. As seen in Table VII the $b\bar{b}$ χ_2 widths are easily explained by the lowest-order theory but the $c\bar{c}$ χ_2 width seems to be about six times larger than the predicted value. Relativistic wave-function effects reduce the discrepancy to a factor of about 4. The theoretical expectation for the χ_{2c} width, even with relativistic wave-function corrections, appears to be significantly below the experimental value.

One explanation which might be advanced for the disagreement between the theoretical and experimental values of the χ_{2c} width might be QCD radiative corrections. These corrections have been calculated[20] in lowest order and, depending on the renormalization point chosen, can be quite large. We thus gain little insight into the total radiative corrections. However, since the χ_{2b} and χ'_{2b} widths are roughly consistent with the leading term we might conclude that the radiative corrections are under control in that they probably do not change the lowest-order width by more than 50%.

Another explanation which can probably be rejected is a massive failure of QCD factorization. The wave functions which appear in Eqs. (17) are normally taken to be the same as the $Q\bar{Q}$ bound-state wave functions. This would not be the case if the initial-state radiative corrections to the decay process are not actually part of the bound-state wave function. Just as in the radiative correction case it would be surprising if the χ_{2b} rate was correctly predicted and the χ_{2c} not due to a breakdown in factorization.

The most reasonable way to account for the failure of the χ width calculation in the c case but not the b case is from relativistic corrections. We have already seen that relativistic kinetic energy corrections alone will increase the χ_{2c} rate by 50%. Spin-dependent relativistic corrections may also increase this rate. With the fortutious collaboration of radiative corrections and a more accurate (and smaller) experimental width measurement, agreement may yet be achieved.

TABLE VII. χ_2 hadronic widths. There is good agreement between the χ_{2b} and χ'_{2b} measured and predicted widths. The χ_{2c} predicted widths are considerably smaller than the measured values. Spin-independent kinetic energy wave-function corrections increase the χ_{2c} width prediction by 50%.

	Cornell		Wisconsin	
	S	SS	S	SS
$\Gamma(\chi_{2b} \to 2g) = 144 \pm 35$ keV (experiment)				
$\lvert R'_p(0)\rvert^2$ (GeV^5)	1.39	1.69	1.51	1.80
$\Gamma(\chi_{2b} \to 2g)$ (keV)				
$\alpha_s = 0.16$	95	115	103	123
$\alpha_s = 0.18$	120	145	130	155
$\Gamma(\chi'_{2b} \to 2g) = 130^{+130}_{-40}$ keV (experiment)				
$\lvert R'_p(0)\rvert^2$ (GeV^5)	1.77	2.28	1.56	1.96
$\Gamma(\chi'_{2b} \to 2g)$ (keV)				
$\alpha_s = 0.16$	105	135	92	116
$\alpha_s = 0.18$	132	171	117	147
$\Gamma(\chi_{2c} \to 2g) = 2.5 \pm 1.0$ MeV (experiment)				
$\lvert R'_p(0)\rvert^2$ (GeV^5)	0.058	0.096	0.073	0.109
$\Gamma(\chi_{2c} \to 2g)$ (MeV)				
$\alpha_s = 0.2$	0.37	0.62	0.47	0.70

SUMMARY

Using two realistic interquark potentials we have compared the predictions of the nonrelativistic (S) and relativistic (SS) wave equations for a range of heavy-quark spectroscopic data. To avoid introducing many theoretical assumptions we consider only spin-averaged energy levels. Our result is that using a relativistic kinetic energy somewhat improves the already satisfactory $c\bar{c}$ and $b\bar{b}$ energy levels and ratios of leptonic widths and that wave-function corrections increase annihilation decay rates and decrease radiative rates as required phenomenologically.

Of particular interest to us are the wave-function corrections induced by relativistic kinematics. In heavy quarkonia the lowest few energy levels are known but the quark masses and the detailed shape of the potential are not. The proper procedure in this case is to adjust the quark masses and the potential so that the observed particle energy levels agree as accurately as possible with the predicted ones using either nonrelativistic or relativistic kinetic energies.

As seen in Figs. 2–9, for distances greater than a few Compton wavelengths the SS and S s-wave and derivative of the p-wave wave functions are virtually identical. Below one or two Compton wavelengths the relativistic s-wave wave functions begin to rise steadily above the S wave functions. The same rise is seen in the derivative of the p-wave wave function. At about one-fifth wavelength the s-wave wave functions and the derivative of the p-wave wave functions rise sharply. This singular behavior can be ascribed to the instantaneous approximation and hence is unphysical.

To separate the relativistic kinematic wave-function enhancement from the spurious wave-function singularity at $r=0$ we employ the sum rules of Eqs. (12) and (13). These sum rules provide an effective S wave function at $r=0$ which then can be used to compute annihilation rates. Radiative (photon) decays are straightforwardly computed as expectation values using either S or SS wave functions. The $r=0$ singularity is wiped out by the p-wave angular momentum barrier factor in this case.

We find that kinematic relativistic corrections decrease the $\chi_J \to \psi\gamma$ transition rates, but not enough to give good

agreement with experiment. Spin-dependent corrections and coupling to the $D\bar{D}$ channel are also expected to be important in this case. A surprising result is that the radiative decay rates between states with no nodes were modified by relativistic corrections as strongly as in transitions where strong cancellations occur.

Two-gluon annihilations are in good agreement with experiment for η_c and χ_{2b} decays but not for χ_{2c} decay. The S wave function considerably underestimates the χ_{2c} decay rate and SS wave function is larger at $r=0$ but only increases the rate by about 50%. Because the χ_b predictions are in reasonable agreement with experiment we expect that relativistic wave-function corrections are the most likely consideration. We have only examined the wave-function corrections due to kinetic energy. A more complete analysis including spin-dependent corrections is currently in progress.

ACKNOWLEDGMENTS

This research was supported in part by the University of Wisconsin Research Committee with funds granted by the Wisconsin Alumni Research Foundation, and in part by the U.S. Department of Energy under Contract No. DE-AC02-76ER00881.

APPENDIX

In this appendix we will review the Rayleigh-Ritz-Galerkin (RRG) method[21] for the solution of a certain class of eigenvalue problems. Consider an eigenvalue problem of the form

$$W(\nabla^2)\psi(\mathbf{r})+V(r)\psi(\mathbf{r})=M\psi(\mathbf{r}) , \tag{A1}$$

where M is the eigenvalue parameter. This general form encompasses the Schrödinger equation, for which

$$W(\nabla^2)=\frac{-\nabla^2}{m}+2m \tag{A2a}$$

and the spinless Salpeter[22] equation for which

$$W(\nabla^2)=2(-\nabla^2+m^2)^{1/2} . \tag{A2b}$$

Here, m denotes the quark mass and for simplicity we only consider the equal-mass case. We define the Fourier transform of a function by

$$\hat{\psi}(\mathbf{p})=\int d^3\mathbf{r}\, e^{i\mathbf{p}\cdot\mathbf{r}}\psi(\mathbf{r}) . \tag{A3a}$$

The inverse transform is given by

$$\psi(\mathbf{r})=\int \frac{d^3\mathbf{p}}{(2\pi)^3} e^{-i\mathbf{p}\cdot\mathbf{r}}\hat{\psi}(\mathbf{p}) . \tag{A3b}$$

Multiplying Eq. (A1) by $e^{i\mathbf{p}\cdot\mathbf{r}}$ and integrating over $\mathbf{r}$, we obtain

$$W(p^2)\hat{\psi}+\hat{V}_*\hat{\psi}=M\hat{\psi} , \tag{A4}$$

where the asterisk product denotes convolution:[23]

$$\hat{V}_*\hat{\psi}\equiv\int \frac{d^3\mathbf{p}'}{(2\pi)^3}\hat{V}(\mathbf{p}-\mathbf{p}')\hat{\psi}(\mathbf{p}') . \tag{A5}$$

Let $\{\hat{e}_1,e_2,\ldots\}$ be an orthonormal basis for $L_2(R^3)$. We seek an approximate solution to Eq. (A4) in the form

$$\hat{\psi}(\mathbf{p})=\sum_{j=1}^{N} C_j\hat{e}_j(\mathbf{p}) , \tag{A6}$$

where the C_j are as yet undetermined coefficients. Substituting Eq. (A6) into Eq. (A4) we obtain

$$\sum_{j=1}^{N} C_j W(p^2)\hat{e}_j+\sum_{j=1}^{N} C_J\hat{V}_*\hat{e}_j-M\sum_{n=1}^{N} C_j\hat{e}_j=0 . \tag{A7}$$

In general, Eq. (A7) cannot be satisfied because Eq. (A6) was only an approximate solution. However, we can require that the left-hand side of Eq. (A7) be orthogonal to each of the N basis functions $\{e_1,e_2,\ldots,e_N\}$. In other words, we require that the projection of Eq. (A7) onto the subspace formed by the span of the N functions $\{e_1,e_2,\ldots,e_n\}$ be satisfied identically. Taking inner products, we obtain

$$\sum_{n=1}^{N} C_j\langle\hat{e}_i,W(p^2)\hat{e}_j\rangle+\sum_{n=1}^{N} C_j\langle\hat{e}_i,\hat{V}_*\hat{e}_j\rangle=MC_i , \tag{A8}$$

for $i=1,2,\ldots,N$. The inner product is denoted by angle brackets:

$$\langle\hat{f},\hat{g}\rangle\equiv\int d^3\mathbf{p}\,\hat{f}(p)\hat{g}(p) . \tag{A9}$$

Define the $N\times N$ matrix A whose ijth entry is given by

$$A_{ij}=\langle\hat{e}_i,W(p^2)\hat{e}_j\rangle+\langle\hat{e}_i,\hat{V}_*\hat{e}_j\rangle . \tag{A10}$$

Then Eq. (A8) becomes

$$\sum_{n=1}^{N} A_{ij}C_j=MC_i,\quad i=1,2,\ldots,N \tag{A11}$$

or in matrix notation

$$AC=MC . \tag{A12}$$

This is an ordinary matrix eigenvalue equation. One can show[21] that the eigenvalues of this matrix equation converge to the eigenvalues of Eq. (A4). Also, the approximate solutions Eq. (A6) with the C_j determined above as eigenvectors of the matrix A will converge to the solutions of Eq. (A4). Furthermore, if the eigenvalue spectrum of Eq. (A4) is positive definite (which will occur for all physically reasonable potentials) then one can show that[21]

$$M_1\le M_1^{(N)},\quad M_2\le M_2^{(N)},\quad M_3\le M_3^{(N)},\ldots, \tag{A13}$$

where the M_i are the exact eigenvalues of Eq. (A4) and the $M_i^{(N)}$ are the eigenvalues of Eq. (A12).

The operator $W(p^2)+\hat{V}_*$ is self-adjoint, so that

$$\langle\hat{e}_i,W\hat{e}_j\rangle+\langle\hat{e}_i,\hat{V}_*\hat{e}_j\rangle=\langle W\hat{e}_i,\hat{e}_j\rangle+\langle\hat{V}_*\hat{e}_i,\hat{e}_j\rangle \tag{A14a}$$

$$=\overline{\langle\hat{e}_j,W\hat{e}_i\rangle}+\overline{\langle\hat{e}_j,\hat{V}_*\hat{e}_i\rangle} , \tag{A14b}$$

where the overbar denotes complex conjugation. Thus

$$A_{ij}=\bar{A}_{ji} \tag{A15}$$

and the matrix A will be Hermitian. We will choose the $\hat{e}_j$ so that A_{ij} is real; A will then be a real symmetric matrix. Thus we will only need to evaluate the diagonal and upper triagonal elements of A. The inner product of $\hat{e}_i$

with a convolution may be easily evaluated by direct substitution into coordinate space quantities:

$$\langle \hat{e}_i, \hat{V}_* \hat{e}_j \rangle = (2\pi)^3 \langle e_i(-\mathbf{r}), V(r) e_j(\mathbf{r}) \rangle , \tag{A16}$$

where $e_i(\mathbf{r})$ is the inverse transform of $\hat{e}_i(\mathbf{p})$. Thus,

$$A_{ij} = \langle \hat{e}_i, W \hat{e}_j \rangle + (2\pi)^3 \langle e_i(-\mathbf{r}), V(r) e_j(\mathbf{r}) \rangle \tag{A17a}$$

$$= \int d^3\mathbf{p}\, \hat{e}_i(\mathbf{p}) W(p^2) \hat{e}_j(\mathbf{p}) + (2\pi)^3 \int d^3\mathbf{r}\, e_i(-\mathbf{r}) V(r) e_j(\mathbf{r}) . \tag{A17b}$$

We choose for basis functions

$$\hat{e}_{jlm}(\mathbf{p}) = (\hat{N}_{jl})^{-1} (mp_1)^{-3/4} \left[\frac{1}{1+4y^2} \right]^{l+2} \times J_{j-1}^{(l+3/2, l+1/2)} \left[\frac{4y^2-1}{4y^2+1} \right] y^l Y_{lm} , \tag{A18}$$

where Y_{lm} is a spherical harmonic;

$$\hat{N}_{jl} = (2\pi)^{1/2} \left[\frac{2^{l+3} \Gamma(\frac{1}{2})}{\Gamma(j+l+\frac{1}{2})} \right] \{ [(j+l+1)!(j-1)!]^{1/2} \}^{-1}$$

is a normalization constant, and

$$J_j^{(l+3/2, l+1/2)} \left[\frac{4y^2-1}{4y^2+1} \right]$$

is the jth Jacobi polynomial[24] of the argument $(4y^2-1)/(4y^2+1)$ with parameters $l+\frac{3}{2}$ and $l+\frac{1}{2}$. The dimensionless variable y is related to $p = |\mathbf{p}|$ by

$$y = \frac{p}{(mp_1)^{1/2}} , \tag{A19}$$

where p_1 is an arbitrary constant. In practice, p_1 is chosen to minimize the approximate eigenvalues obtained from Eq. (A12) since the approximate eigenvalues are always larger than the true eigenvalues. The inverse transforms of the basis functions are given by[25]

$$e_{jlm}(\mathbf{r}) = \frac{(-i)^l}{(2\pi)^{3/2}} (mp_1)^{-3/4} N_{jl}^{-1} e^{-x/2} L_{j-1}^{(2l+2)}(x) x^l Y_{lm} \tag{A20}$$

where

$$N_{jl} = \left[\frac{(j+2l+1)!}{(j-1)!} \right]^{1/2} \tag{A21}$$

is a normalization constant, $L_j^{(2l+2)}(x)$ is the jth generalized Laguerre polynomial[24] with parameter $2l+2$ and x is related to $r = |\mathbf{r}|$ by

$$x = r(mp_1)^{1/2} . \tag{A22}$$

Substituting these basis functions into Eq. (A17b) and using the orthonormality of the spherical harmonics, we find

$$A_{ij} = \int_0^\infty W(p^2) \left[\frac{1}{1+4y^2} \right]^{2l+4} y^{2l+2} \frac{J_{i-1}}{N_{il}} \frac{J_{j-1}}{N_{jl}} dy + \int_0^\infty V(r) x^{2l+2} e^{-x} \frac{L_{i-1}}{N_{il}} \frac{L_{j-1}}{N_{jl}} dx . \tag{A23}$$

By making the change of variable $z = (4y^2-1)/(4y^2+1)$, the first integral may be simply evaluated using Gauss-Chebyshev quadrature.[26] The second integral can be evaluated using Gauss-Laguerre quadrature.[26] Once the A_{ij} have been evaluated, the eigenvalues and eigenvectors of the matrix can be obtained by using standard methods for determining the eigensystems of real symmetric matrices.[26,27]

[1] T. Appelquist, R. M. Barnett, and K. D. Lane, Annu. Rev. Nucl. Part. Sci. **28**, 387 (1978); J. L. Richardson, Phys. Lett. **82B**, 272 (1979); W. Buchmüller and S.-H. H. Tye, Phys. Rev. D **24**, 132 (1981).

[2] E. Eichten, K. Gottfried, T. Kinoshita, K. D. Lane, and T. M. Yan, Phys. Rev. D **17**, 3090 (1978); **21**, 203 (1980).

[3] A. Martin, Phys. Lett. **93B**, 338 (1980).

[4] K. J. Miller and M. G. Olsson, Phys. Rev. D **25**, 2383 (1982).

[5] Kaoru Hagiwara, Steve Jacobs, M. G. Olsson, and K. J. Miller, Phys. Lett. **131B**, 455 (1983).

[6] D. P. Stanley and D. Robson, Phys. Rev. D **21**, 3180 (1980); L. Hostler and W. Repko, Ann. Phys. (N.Y.) **130**, 329 (1980); Stephen Godfrey and Nathan Isgur, Phys. Rev. D **32**, 189 (1985); L. J. Nickisch, L. Durand, and B. Durand, Phys. Rev. D **30**, 660 (1984).

[7] Bernice Durand and Loyal Durand, Phys. Rev. D **25**, 2312 (1982).

[8] Bernice Durand and Loyal Durand, Phys. Rev. D **30**, 1904 (1984).

[9] Loyal Durand, Phys. Rev. D **32**, 1257 (1985).

[10] Godfrey and Isgur (Ref. 6).

[11] C. Quigg and J. L. Rosner, Phys. Rep. **56**, 167 (1979); Avinash Khare, Nucl. Phys. **B152**, 533 (1979).

[12] Richard McClary and Nina Byers, Phys. Rev. D **28**, 1692 (1983).

[13] T. Appelquist and H. D. Politzer, Phys. Rev. Lett. **34**, 43 (1975); A. DeRújula and S. L. Glashow, *ibid.* **34**, 46 (1975); R. Barbieri, R. Gatto, and R. Kögerler, Phys. Lett. **60B**, 1976 (1976); V. A. Novikov, L. B. Okun, M. A. Shifman, A. I. Vainshtein, M. B. Voloshin, and V. I. Zakharov, Phys. Rep. **41C**, 1 (1978); E. Remidi, in *Theory of Fundamental Interactions,* proceedings of the International School of Physics, "Enrico Fermi," Course 81, Varenna, 1980, edited by G. Costa and R. R. Gatto (North-Holland, Amsterdam, 1980).

[14] G. P. Lepage, in *Proceedings of the 1983 International Symposium on Lepton and Photon Interactions at High Energy, Ithaca, New York,* edited by D. G. Cassel and D. L. Kreinick (Newman Laboratory of Nuclear Studies, Cornell University, 1983).

[15] M. G. Olsson, A. D. Martin, and A. W. Peacock, Phys. Rev.

D 31, 81 (1985).

[16]D. Hitlin, in *Proceedings of the 1983 International Symposium on Lepton and Photon Interactions at High Energy, Ithaca, New York* (Ref. 14).

[17]C. Baglin *et al.*, contribution to the VII European Symposium on Antiproton Interactions, Durham, England, 1984 (unpublished); A. Silverman, in *Proceedings of the XXII International Conference on High Energy Physics, Leipzig, 1984,* edited by A. Meyer and E. Wieczorek (Akademie der Wissenschaften der DDR, Zeuthen, DDR, 1984); M. Macri and A. Lundby (private communication).

[18]M. Oreglia (private communication); a similar width is obtained from the $\chi_2 \rightarrow \psi\gamma$ branching ratio and a calculation of the radiative decay rate (see Ref. 15).

[19]Juliet Lee-Franzini, in *Physics in Collision V,* proceedings of the Fifth International Conference, Autun, France, 1985, edited by B. Aubert and L. Montanet (Editions Frontiéres, Gif-sur-Yvette, France, 1985).

[20]R. Barbieri, M. Caffo, R. Gatto, and E. Remiddi, Phys. Lett. **95B**, 93 (1980).

[21]I. Stakgold, *Green's Functions and Boundary Value Problems* (Wiley, New York, 1984).

[22]Stanley and Robson (Ref. 6); Godfrey and Isgur (Ref. 6); Durand, Durand, and Nickish (Ref. 6).

[23]Strictly speaking, Eq. (A5) is only valid when $V(r)$ is square integrable. However, if $e^{-\epsilon r}V(r)$ is square integrable (and we will only consider potentials for which this holds) then we may replace Eq. (A5) with

$$\hat{V}_* \hat{\psi} \equiv \lim_{\epsilon \to 0} \int \frac{d^3\mathbf{p}'}{(2\pi)^3} \hat{V}_\epsilon(\mathbf{p}-\mathbf{p}')\hat{\psi}(\mathbf{p}') ,$$

where $\hat{V}_\epsilon \equiv \int d^3\mathbf{r}\, e^{i\mathbf{p}\cdot\mathbf{r}} e^{-\epsilon r} V(r)$. In either case, Eq. (A16) remains valid.

[24]M. Abramowitz and I. Stegun, *Handbook of Mathematical Functions* (Dover, New York, 1965).

[25]E. Joachin Weniger, J. Math. Phys. **26**, 276 (1985).

[26]A. Ralston and P. Rabinowitz, *A First Course in Numerical Analysis* (McGraw-Hill, New York, 1978).

[27]J. H. Wilkinson and C. Reinsch, *Linear Algebra: A Handbook for Automatic Computation* (Springer, Berlin, 1971).